

Evaluation of Monument Stability in the SWEPOS GNSS Network using Terrestrial Geodetic Methods – up to 2003

Martin Lidberg

Mikael Lilje

Gävle 2007

L A N T M Ä T E R I E T





Copyright ©

2007-09-25

Författare Martin Lidberg, Mikael Lilje

Typografi och layout Rainer Hertel

Totalt antal sidor 42

LMV-rapport 2007:10 – ISSN 280-5731

Evaluation of Monument Stability in the SWEPOS GNSS Network using Terrestrial Geodetic Methods – up to 2003

Martin Lidberg

Mikael Lilje

Gävle 2007

LANTMÄTERIET



Evaluation of Monument Stability in the SWEPOS GNSS Network using Terrestrial Geodetic Methods – up to 2003

1	Introduction	7
1.1	Thermal deformation	8
1.2	Local control networks	10
1.3	Purpose of this report	12
2	Pillar top measurements	14
3	Results of pillar measurements	17
4	Discussion	23
5	Acknowledgements	27
6	References	27
A.	Pillar displacement due to thermal bending	29

B.	Leica TDA5005 - GDM 440 instrument height difference	32
C.	T2 - GDM440 instrument heights	33
D.	Plots of measured displacements of the pillar reference point	34

Evaluation of Monument Stability in the SWEPOS GNSS Network using Terrestrial Geodetic Methods – up to 2003

1 Introduction

The SWEPOS™ network of GNSS reference stations began as a co-operation between Lantmäteriet (the National Land Survey of Sweden) and Onsala Space Observatory in the beginning of the 1990's. The early design phase of SWEPOS occurred during 1992. It was stated that the purpose of the network was both scientific and practical, to the benefit of professional users and to the public. It is the purpose of SWEPOS to (Jonsson et al. 2006):

- Provide L1 and L2 raw data to post-processing users
- Provide DGNSS and RTK corrections to real-time users
- Act as high-precision control points for Swedish GPS users
- Provide data for scientific studies of crustal motion
- Monitor the integrity of the GPS/GLONASS system.

SWEPOS is also the basis for the Swedish national reference frame, SWEREF 99 (Jivall & Lidberg 2000, Jivall 2001).

At the start in August 1993, SWEPOS consisted of 20 stations covering Sweden with an approximate inter-station distance of 200 km (the 21st station, SPT0, was added in December 1995), see figure 1.

In order to be a useful observing system for the study of crustal deformations as well as a firm foundation for the geodetic reference frame, the monuments that carry the GNSS antennas were already in the first planning phase recognised as a key component of SWEPOS. The standard SWEPOS monument, used at most of the 21 original sites, is a 3 m tall reinforced concrete pillar anchored into crystalline rock. Exceptions are Lovö, Mårtsbo, and Onsala, which all have a long history as geodetic stations. Jönköping has a standard SWEPOS pillar, but only 1 m tall. In order to reduce deformation of the pillar due to thermal expansion, resulting in displacements of the pillar top, the pillars are insulated and electrically temperature stabilized to a temperature above 15°C, see Figure 2.

For the early history of SWEPOS, see Hedling and Jonsson (1993).

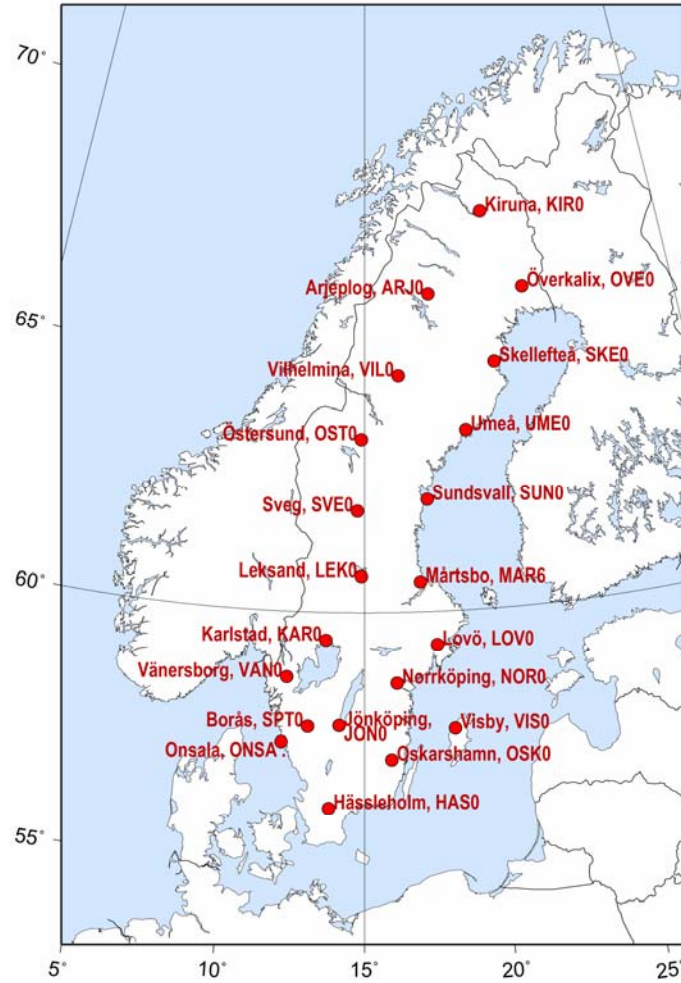


Figure 1. The 21 SWEPOS stations considered in this study. Stations are labelled with both names and their 4 character abbreviations.

1.1 Thermal deformation

Thermal expansion

The thermal expansion of a 3 meter concrete pillar may be calculated as (Björk 1981):

$$\Delta l = l \cdot \alpha \cdot \Delta t \quad (1)$$

where Δl is the thermal expansion, l is the length of the material, α is the thermal expansion coefficient, and Δt is change of temperature. The length (height) of the pillar is about 3 meters, a value of $12 \cdot 10^{-6} \text{ K}^{-1}$ may be used as thermal expansion coefficient for concrete and steel (Nordling and Österman 2004), and the difference between minimum and maximum temperature can be estimated to a value of 50 K (-25 to 25 °C in the north, and -20 to +30 in the south),

which may be somewhat low to the north and high to the south. These values yield an expansion of 1.8 mm.

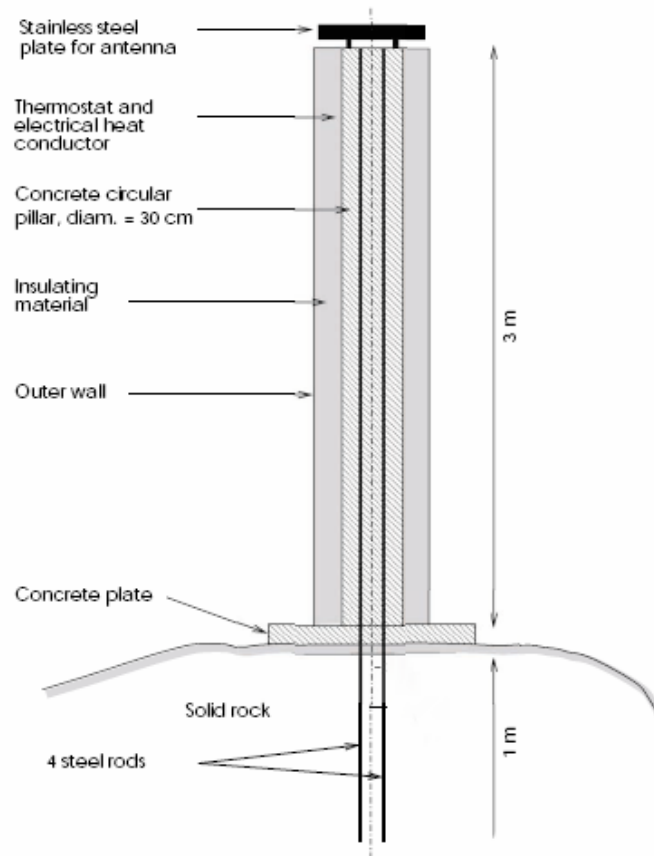


Figure 2. Sketch of the standard SWEPOS pillar. From Scherneck et al (2002).

This 2 mm change in height (peak-to-peak) of the pillar was the main argument for the insulating and the electrically temperature stabilizing of the monuments.

Thermal bending

If the deformation of the pillar would follow the simple rule described above, the 2 mm change in height would be bad but perhaps not extremely critical. However, a non-insulated pillar may be subjected also to bending caused by different temperatures on different sides of the pillars – e.g. due to unequal heating from sunshine. Such bending would cause motion of the top of the pillar in the horizontal components, and thus horizontal displacement of the GNSS antenna.

In Appendix A is given a theoretical derivation of what we may call the “bending displacement equation”:

$$\Delta x = \frac{l^2}{2} \cdot \frac{\alpha}{D} \cdot \Delta t \quad (2)$$

where Δx is the horizontal displacement of the pillar top, l is the height of the pillar (3 m for standard SWEPOS pillar), D is the diameter of the concrete pillar (here 30 cm), and Δt is the temperature difference between the warm and cold sides of the pillar. The thermal expansion coefficient, α is again $12 \cdot 10^{-6} \text{ K}^{-1}$ for concrete and steel.

A quantitative estimate of horizontal displacement due to pillar bending for some realistic (?) temperature differences are given in Table 1.

Table 1. Example of thermal bending displacements for a concrete pillar without insulation.

Temperature difference (K)	$\Delta x = \frac{3^2}{2} \cdot \frac{12 \cdot 10^{-6}}{0.3} \cdot \Delta t$ (m)	Horizontal displacement (mm)
1	$\Delta x = 0.00018 \cdot 1$	0.18
2	$\Delta x = 0.00018 \cdot 2$	0.36
5	$\Delta x = 0.00018 \cdot 5$	0.9
10	$\Delta x = 0.00018 \cdot 10$	1.8

1.2 Local control networks

In the design of SWEPOS as an observing system for scientific purposes, it was concluded that it should be possible to measure motions of the pillar top with respect to the surrounding bedrock. Therefore a small high-precision geodetic network was established around each pillar. The procedure for measuring the position of the pillar top is to remove the GNSS antenna and replace it with a theodolite or a total station. The positioning is then performed by resection of the geodetic instrument by observing the horizontal and vertical angles to the markers in the network. The networks usually consist of 5 steel bolts (figure 3) driven into the rock, in such a way that their tops protrude a few centimetres above the surface. The centre of the steel bolt is marked by a bore hole of 2 mm diameter. The networks typically have an extension of 10 to 20 meters (figure 4).

Figure 5 and 6 show photos of SWEPOS stations while establishing the local network, and while performing the pillar measurement.



Figure 3. A 20 mm steel bolt anchored about 1 dm into the rock and used as monument in the local geodetic network.

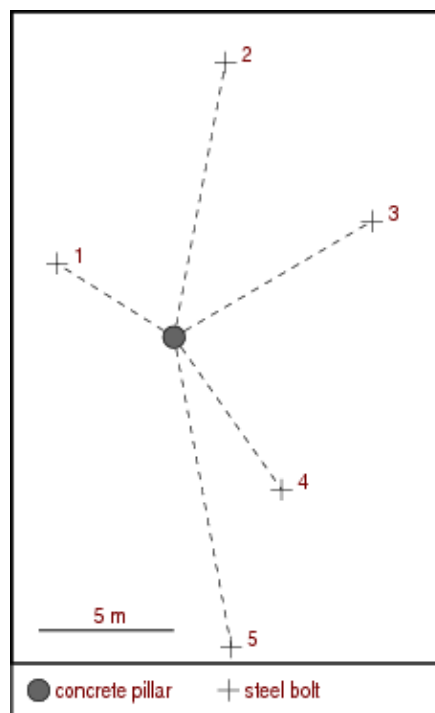


Figure 4. Sketch of the local geodetic network at the SWEPOS station Leksand.



Figure 5. Picture from a SWEPOS station while establishing the local network. This pillar is not insulated. (The photo is from Sikskär – now SWEPOS station “Holmsund”, which was however not included in the original 21 SWEPOS stations.)



Figure 6. Picture from Leksand, during pillar top measurement.

1.3 Purpose of this report

The purpose of this report is to compile the results of the pillar-measurements performed at the 21 “original” SWEPOS monuments so far – to give an indication if there are any significant motions of the pillar top relative to the bedrock. Because the pillar-

measurements include a remove-and-replace procedure, there is a potential risk that the pillar-measurements cause small shifts in the GNSS position time series. Solving for such shifts while estimating station velocities, weakens the accuracy in the estimated velocity considerably. A very important question is therefore whether further pillar-measurements should be performed or not.

2 Pillar top measurements

In this study we analyze the co-ordinate changes of the reference points of the monuments, with respect to the local networks as achieved from the local pillar top measurements. This reference point is materialized as a bore hole in the steel plate at the top of the pillar, used for attaching the GNSS antenna. More precisely, it is the centre of the upper part of the bore hole at the level of the surface of the steel plate. In SWEPOS these points are denoted "Pillar Plate", in short PP. See Figure 7. The GNSS antennas are attached to the pillar top through a tribrach (where one of the foot screws is always lowered to its bottom position to keep the distance from PP to antenna reference point – ARP – constant), and an adapter.

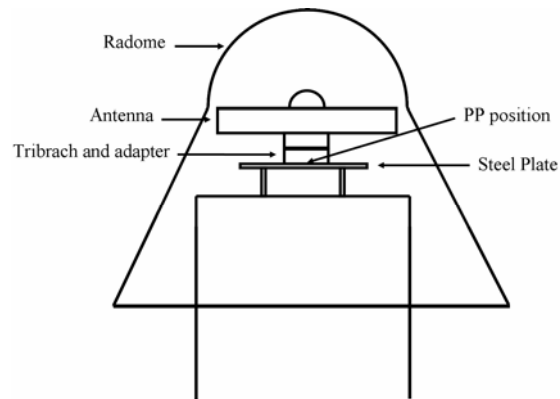


Figure 7. Sketch of the pillar top with an attached GNSS antenna and covered by a radome.

The pillar measurements are performed using terrestrial geodetic observations. The antenna and the adapter are removed from the tribrach and replaced by a theodolite or, preferably, a modern total station. The position determination is performed as a so called "free station" of the instrument, by measuring only horizontal and vertical angles to the markers in the local network. For the following weighted least squares adjustment (where the steel bolt markers in the local networks are kept fixed), a modified version of the survey field computer program AutoKa-FC (in-house software from Lantmäteriet) was used for the pillar measurements carried out up to 1999, and the STAR*NET-PLUS Version 6 (from Starplus software, Inc) was used for the 2003 measurements.

The measurements up to year 1999 were carried out with the use of a Geodimeter type 440 (hereafter denoted GDM440), and a Leica TDA 5005 was used for the 2003 measurements. To get a consistent series

of pillar measurements, and not introducing shifts (most likely in the vertical component) due to the change of instrument, the difference in instrument heights must be known. This difference was estimated to 22.11 mm (Geodimeter higher than Leica). The method was to read a levelling rod (in two faces) from, in turn, the Geodimeter and the Leica instrument attached to the same tribrach. The (somewhat relaxed) notes from the calibration are found in Appendix B.

Some early pillar measurements were carried out using the Wild T2 type theodolite. Results from the determination of instrument height differences between the T2 and GMD440 instruments are given in Appendix C.

Angle observations at short target distances, using modern survey instruments, have the potential to give a very accurate point determination. The applied method for pillar measurement is therefore supposed to result in position uncertainties at the fraction of a millimetre (standard error). A rough estimation may be as follows:

- Standard error in observation of directions: 1 mgon. A pessimistic estimate of distance to target to 10 meters results in a linear standard error of 0.16 mm.
- Standard error in pointing to target: 0.1 mm
- Standard error in centring of the instrument, when it replaces the GNSS-antenna in the tribrach using the forced centring method: 0.15 mm.

Quadratic addition gives a total standard error of 0.24 mm. Here it may be noted that this estimate is supposed to be somewhat pessimistic. The error in position, caused by errors in observed directions and by pointing error, is reduced in the least squares adjustment when we use redundant observations. The centring error is however not reduced.

We can also find an estimate of the uncertainty in the pillar measurements by analysing the standard error in the computed position from the least squares adjustment. Table 1 shows the a posteriori standard errors in the north, east and up components from the adjustment of measurements made in 2003. The mean values of the achieved standard errors in the position determination are 0.15, 0.16 and 0.17 mm for the north, east and up components respectively. The table also contains the values of the semi-major and semi-minor axes of the horizontal error ellipses at the 95% confidence level. Quadratic adding of the error ellipses semi-axes (and dividing by 2 - approximate value - to change from the 95% confidence level, to the 1 σ level) gives a position standard error of 0.28 mm, close to the above estimated total standard error (0.24 mm).

Table 1. Estimated uncertainty in pillar top position achieved from the weighted least squares adjustment of the pillar measurements carried out in 2003.

Pillar	a posteriori standard error of computed position			error ellipse (mm) (95% confidence level)	
	North (mm)	East (mm)	Up (mm)	semi-major axis	semi-minor axis
arj0	0.14	0.14	0.16	0.35	0.34
spt0	0.15	0.16	0.17	0.44	0.33
has0	0.15	0.17	0.17	0.42	0.36
jon0	0.16	0.18	0.16	0.46	0.36
kar0	0.16	0.16	0.17	0.39	0.38
kir0	0.15	0.17	0.17	0.43	0.35
lek0	0.18	0.13	0.15	0.44	0.31
lov0			0.25		
Mårtsbo S	0.15	0.20	0.16	0.52	0.33
nor0	0.16	0.16	0.17	0.41	0.36
onsa					
osk0	0.14	0.14	0.16	0.36	0.32
ost0	0.17	0.19	0.19	0.53	0.34
ove0	0.15	0.14	0.15	0.38	0.33
ske0	0.15	0.26	0.17	0.67	0.32
sun0	0.15	0.13	0.15	0.37	0.32
sve0	0.13	0.15	0.16	0.38	0.31
ume0					
van0	0.14	0.13	0.19	0.37	0.31
vil0	0.14	0.14	0.16	0.35	0.32
vis0	0.18	0.16	0.17	0.44	0.38
RMS ^a :	0.15	0.16	0.17	0.44	0.34
H-RMS ^b	0.22			0.56	

^a Root Mean Square of the values in the columns above.

^b Horizontal value, $\sqrt{a^2 + b^2}$

The differences between the error ellipses semi-axes are in general small, indicating a good geometry in the network and a well conditioned adjustment problem to solve. At Skellefteå (ske0) and Östersund (ost0) the semi-major axis are larger. At both these sites only 4 steel bolts in the local network was used for the position determination. The Skellefteå station is equipped with two piers and the ske0 pillar is located very close to the instrument hut. Therefore it was only possible to use 4 targets. The instrument hut at the Östersund station has been extended in order to facilitate absolute gravimeter observations. After the extension of the hut, one marker can not be used anymore.

A thorough analysis of SWEPOS monument stability based on pillar measurements performed up to 1995 is found in Johansson et al (2002).

3 Results of pillar measurements

Results of the pillar measurements are given in Table 2. The presented north and east coordinates are usually given in the coordinate frame defined by the local geodetic network. The origin of coordinates was defined by the pillar plate position (PP) at the epoch when the local network was determined. Exceptions are Kiruna, where the coordinate frame was defined by a second pillar at the site, and Mårtsbo S, where origin was located in Mårtsbo N. The height value is usually given relative to the first determination.

In this study, we are interested in the stability of the pillar top with respect to the surrounding rock. Thus, we are interested in the scatter within the sample, rather than the absolute values of the PP coordinates. Therefore the stochastic displacements are given as standard deviations (i.e. scatter relative to the mean value of the samples).

Plots of the measured pillar displacements are presented in Appendix D.

Table 2. Results from terrestrial pillar measurements.

Station Pillar	Date	Instr.	Pillar Plate Position (PP) ^a		
			North (mm)	East (mm)	Up (mm)
Arjeplog arj0	1993-08-16	GDM440	-0.16	0.21	0.00
	1996-10-01	GDM440	0.94	0.54	-0.36
	1999-06-11	GDM440	1.26	0.21	-0.74
	2003-10-21	Leica	0.67	0.55	-0.94
	std		0.61	0.19	0.41
Hässleholm has0	1993-06-14	GDM440	0.00	0.00	0.00
	1995-05-19	GDM440	-0.01	-0.22	-0.42
	1996-10-01	GDM440	-0.05	1.16	-0.47
	1999-07-02	GDM440	0.20	-0.08	-0.04
	2003-03-27	Leica	0.42	-0.15	-1.01
std		0.20	0.58	0.41	
Jönköping jon0	1992-07-01	insulation	0.00	0.00	
	1993-06-18	GDM440	0.01	0.04	0.00
	1994-06-23	GDM440	0.03	-0.07	-0.08
	1994-06-23	GDM440	0.00	-0.15	-0.13
	1995-05-21	GDM440	-0.19	-0.23	0.03
	1996-10-01	GDM440	-0.19	-0.33	0.03
	1999-07-05	GDM440	-0.04	-0.49	0.58
	2003-03-28	Leica	-0.08	-0.31	-0.03
std		0.09	0.18	0.24	

Karlstad kar0	1992-07-09	T2	0.00	0.00		
	insulation					
	1993-08-12	T2	0.20	0.03	0.00	
	1995-05-23	GDM440	0.04	0.56	0.70	
	1996-10-01	GDM440	0.15	0.31	-1.45	
	1999-07-07	GDM440	0.26	0.15	-0.80	
	2003-03-31	Leica	0.54	0.00	-1.48	
std		0.19	0.22	0.95		
Kiruna kir0	1993-08-16	GDM440	0.00	0.00	0.00	
	insulation					
	1994-06-15	GDM440	0.11	-0.27	0.12	
	1994-06-15	GDM440	0.02	-0.15	0.10	
	1995-06-16	GDM440	0.01	-0.26	0.41	
	1999-05-12	GDM440	0.32	-0.92	0.48	
	2003-10-20	Leica	-0.93	-0.54	-0.45	
std		0.43	0.33	0.33		
Leksand lek0	1992-07-01		0.00	0.00		
	insulation					
	1993-08-11	T2	-0.26	-0.25	0.00	
	1994-01-18	GDM440	-0.28	0.06	-1.21	
	1994-01-18	GDM440	-0.28	0.12	-1.19	
	1994-02-06	GDM440	-0.33	0.14	-0.75	
	1994-02-06	GDM440	-0.33	0.11	-0.88	
	1994-03-08	GDM440	-0.43	0.10	-0.87	
	1994-03-08	GDM440	-0.43	0.16	-0.91	
	1994-04-15	GDM440	-0.58	0.22	-0.79	
	1994-04-15	GDM440	-0.59	0.18	-0.94	
	1994-06-14	GDM440	-0.42	-0.34	-0.65	
	1994-08-25	GDM440	0.25	-0.36	-0.58	
	1994-08-25	GDM440	0.26	-0.30	-0.60	
	1995-10-05	GDM440	-0.36	0.15	-0.42	
	1996-10-01	GDM440	0.00	0.39	-0.57	
	1999-06-22	GDM440	0.19	-0.28	0.08	
	2003-11-07	Leica	-0.52	0.13	-0.46	
	std		0.28	0.23	0.36	
	Lovo lov0	1993-10-28	GDM440	-0.54	-0.50	0.00
1995-05-16		GDM440	-0.53	-0.22	0.03	
1996-10-01		GDM440	-0.84	-0.42	0.05	
1999-06-28		GDM440	-0.22	-0.36	0.41	
2003-04-02		Leica	-0.70	-0.09	-1.16	
std		0.23	0.16	0.60		
Mårtsbo N mar6	1993-08-05	GDM440	0.66	0.78	0.00	
	insulation					
	1995-10-06	GDM440	0.10	0.57	-0.99	
	1996-11-22	GDM440	0.17	0.47	-1.49	
std		0.35	0.22	1.05		

Mårtsbo S	1993-08-05		0.00	0.00	0.00
	insulation				
	1995-10-06		0.28	-0.76	-0.86
	2003-03-20	Leica	0.71	-0.80	-1.85
	std		0.36	0.45	0.93
Norrköping nor0	1993-06-12	GDM440	0.00	0.00	
	1993-08-22	T2	-0.07	-0.05	0.00
	1994-06-29	GDM440	0.54	0.48	-0.13
	1994-06-29	GDM440	0.42	0.31	-0.26
	1995-05-17	GDM440	0.29	0.30	-0.73
	1996-10-01	GDM440	0.02	0.06	-1.08
	1999-06-29	GDM440	-0.18	0.77	-0.49
	2003-03-25	Leica	-0.46	0.80	-1.21
	std		0.33	0.33	0.47
Onsala onsa	1992-06-16		0.00	0.00	
	1993-08-16		0.14	-0.49	
	1995-05-20		0.45	-0.08	
	2003-03-29	Leica	0.82	-0.42	
	std		0.36	0.24	
Oskarshamn osk0	1993-06-16	GDM440	-0.06	0.02	0.00
	1995-05-18	GDM440	-0.11	-0.24	-0.70
	1996-10-01	GDM440	0.32	-0.54	-0.29
	1999-07-01	GDM440	0.67	-0.70	0.15
	2003-03-27	Leica	0.92	-0.33	-0.24
	std		0.45	0.28	0.32
Östersund ost0	1993-08-10	GDM440	-1.04	0.28	0.00
	1995-09-15	GDM440	-0.19	0.01	0.35
	1996-10-01	GDM440	-0.17	-0.10	0.38
	1999-06-15	GDM440	-0.36	0.02	0.98
	2003-10-23	Leica	-0.96	0.21	0.16
	std		0.42	0.16	0.37
Överkalix ove0	1993-08-19	GDM440	0.00	0.00	
	1994-06-15	GDM440	0.52	0.41	0.00
	1994-06-15	GDM440	0.47	0.30	-0.15
	1995-06-16	GDM440	0.47	1.06	-0.28
	1996-10-01	GDM440	0.27	0.36	1.16
	1999-06-10	GDM440	0.90	1.00	-0.42
	2003-10-19	Leica	0.11	1.20	-1.60
	std		0.30	0.46	0.88
Skellefteå ske0	1992-06-16	T2	0.00	0.00	
	insulation				
	1993-08-15	GDM440	-0.37	0.43	0.00
	1995-06-15	GDM440	-0.61	0.25	0.05
	1996-11-02	GDM440	-0.20	0.38	-0.32
	1999-06-09	GDM440	-0.58	-0.40	0.22
2003-10-18	Leica	1.54	-1.75	0.50	
	std		0.81	0.83	0.30

Borås spt0	1996-08-22	GDM440	0.00	0.00	0.00
	1999-07-04	GDM440	-0.16	-0.11	-0.14
	2003-03-28	Leica	0.72	-0.70	-0.73
	std		0.47	0.38	0.39
Sundsvall sun0	1993-08-09	GDM440	-0.09	-0.30	0.00
	1995-06-13	GDM440	0.75	-1.39	-0.12
	1996-10-01	GDM440	0.91	-2.19	-0.34
	1999-06-08	GDM440	0.77	-1.33	-0.45
	2003-11-05	Leica	0.74	-2.14	-0.95
std		0.40	0.77	0.37	
Sveg sve0	1993-08-03	GDM440	0.03	-0.01	0.00
	1995-06-21	GDM440	-0.07	0.09	-0.02
	1996-10-01	GDM440	-0.03	0.14	-0.19
	1999-06-16	GDM440	1.08	-0.11	1.27
	2003-10-24	Leica	0.89	0.40	-0.05
std		0.56	0.19	0.60	
Umeå ume0	1993-06-13	GDM440	0.00	0.00	0.00
	1995-06-14	GDM440	-0.54	-0.67	2.27
	1996-10-01	GDM440	-0.12	0.38	2.48
	1999-06-08	GDM440	-0.03	1.05	3.88
	2003-11-06	Leica	-0.23	0.28	3.93
std		0.22	0.62	1.60	
Std 95-03.		0.22	0.71	0.89	
Vänernsberg van0	1993-09-09	GDM440	0.38	0.60	0.00
	1995-05-22	GDM440	-0.26	0.37	-0.31
	1996-10-01	GDM440	-0.17	0.80	1.29
	1999-07-06	GDM440	0.32	0.75	0.29
	2003-03-30	Leica	0.62	0.35	-0.42
std		0.38	0.21	0.68	
Vilhelmina vil0	1993-08-11	GDM440	0.04	-0.06	0.00
	1995-06-18	GDM440	-0.44	-0.89	-0.87
	1996-10-01	GDM440	-0.27	-0.97	-1.03
	1999-06-14	GDM440	-0.34	-0.69	-0.91
	2003-10-22	Leica	-0.30	-0.74	-1.09
std		0.18	0.36	0.45	
Visby vis0	1993-08-12	T2	-1.87	1.32	0.00
	1995-06-24	GDM440	-1.52	1.15	-1.23
	1996-05-05	GDM440	-1.90	0.98	-1.56
	1996-05-05	GDM440	-1.91	0.95	-1.54
	1996-10-01	GDM440	0.37	-0.17	-1.35
	1999-06-30	GDM440	0.38	-0.49	-0.99
	2003-03-26	Leica	-1.33	0.76	-1.78
std		1.04	0.69	0.59	

^a North and east coordinates are in the local geodetic network reference frame. Up are usually relative to the first observation. Coordinates of Mårtsbo S and kir0 are also relative to the first observation.

To obtain measures of the average scatter of pillar top displacements for the stations in the SWEPOS network, the “pooled” standard deviations have been computed. The results are given in Table 3.

Table 3. “Pooled” standard deviations of the monument coordinates in Table 2.

	σ_{north} (mm)	σ_{east} (mm)	$\sqrt{\sigma_{\text{north}}^2 + \sigma_{\text{east}}^2}$	up (mm)
“pooled” standard deviation ^{a,b}	0.45	0.42	0.61	0.57

^a Computed as: $\sigma_{\text{pooled}} = \sqrt{(\sum \sigma_i^2 \cdot n_i) / \sum n_i}$, where n_i is number of pillar measurements performed at SWEPOS site i .

^b The observation at ume0 in 1993 has been removed.

The horizontal and vertical residuals (from the mean of the sites samples) are plotted in ascending order in Figure 8 and 9 respectively.

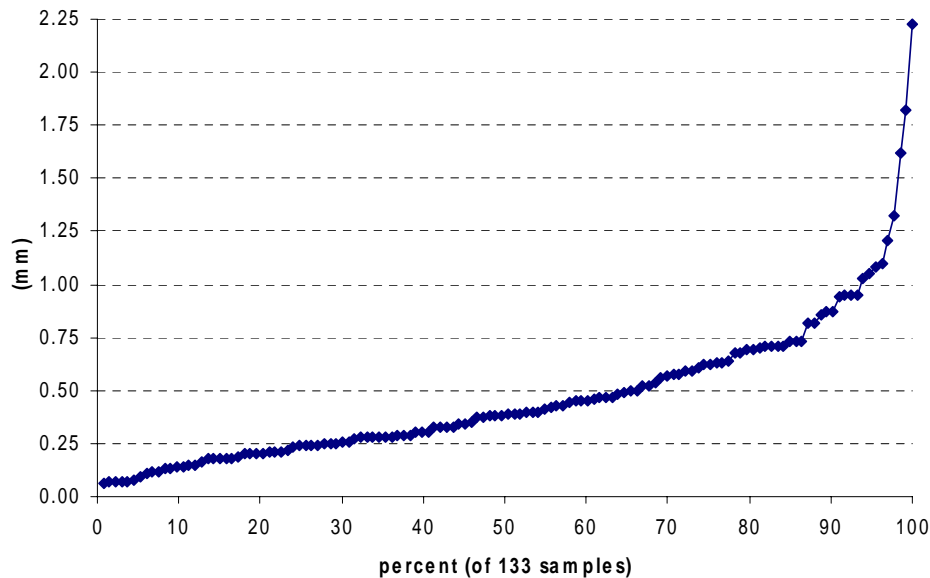


Figure 8. Horizontal residuals in millimetre (from the mean of the samples of the sites) plotted in ascending order against the internal percentage value.

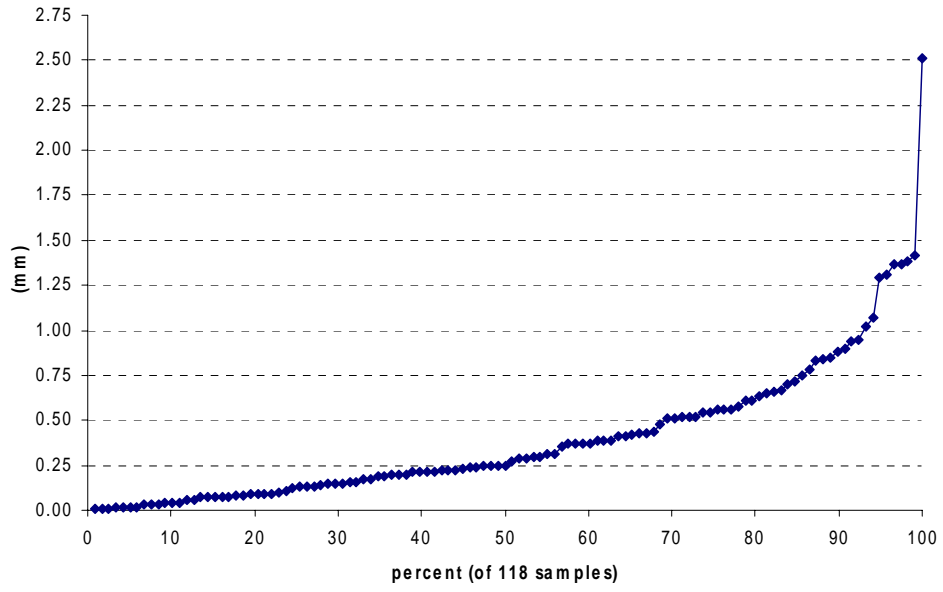


Figure 9. Vertical residuals in millimetre (from the mean of the samples of the sites) plotted in ascending order against the internal percentage value.

4 Discussion

The purpose of this study is to judge whether there is any significant instability of the monuments in the SWEPOS network, with respect to the surrounding rock. Considering the average standard error of the measured pillar top displacements (0.6 mm in both the horizontal and vertical components), it may be concluded that the possible instabilities are small.

Comparing the achieved displacement values with the estimated uncertainty in the measurements (0.2-0.3 mm horizontal and 0.2 mm vertical, 1σ), we conclude that the displacement values do describe real motions of the pillars. The observed motions are only to a limited extent contaminated by measuring errors. This conclusion is further supported by the results of repeated pillar measurements performed within one day. Such double measurements have been done at *kir0*, *lek0*, *nor0*, *ove0*, and *vis0* and the differences are usually within 0.1 mm, sometimes reaching 0.2 mm (see Table 2). Also the small displacements observed at *jon0*, which has a pillar only 1 m tall, support this conclusion.

In order to simplify the discussion on observed motions at individual sites, the maximum (peak-to-peak) scatter in horizontal and vertical positions at each site (these plots are shown in Appendix D) is presented in Table 5. Classification has been done by checking if the samples in the horizontal scatter plot fit within a square with side length 1, 1.5 or 2 (mm) respectively, and similar for the vertical component.

It is noted that only 6 sites (*jon0*, *onsa*, *osk0*, (*ost0*), *spt0*, and *vil0*) fall within 1 mm for both horizontal and vertical components. We note that *onsa* and *jon0*, which have low monuments (1 m), both belong to this group. Additional 8 sites (*arj0*, *has0*, *kir0*, *lek0*, *lov0*, *mar6*, *nor0*, *sve0*) fall within the 1.5 mm limit. However, the horizontal position at 4 of these sites fulfils the 1 mm limit, and 3 sites pass the vertical 1 mm limit. Remaining sites are *kar0*, *ove0*, *ske0*, *sun0*, *ume0*, *van0* and *vis0*.

The vertical component at *kar0* and *van0* shows a scatter of 2 mm, and at *ove0*, we have 3 mm. No explanations have been found so far. However, if the measurement 1999 at *vil0* is excluded, the remaining measurements fall within 1 mm. At *ske0* the horizontal displacement is almost 3 mm. If the measurement 2003 is excluded the remaining 5 measurements fall within the 1 mm box. However, no evidence for gross error in the measurements or computation is found. For *sun0* we have a horizontal scatter of 2 mm. This decreases to 1 mm box if the first measurement in 1993 is excluded.

Table 5. Compilation of maximum scatter of measured pillar top positions at each site shown in Appendix D.

Station	Horizontal position within ^a (mm)	Vertical position within ^b (mm)	Comments
arj0	1.5	1	
has0	1.5	1	
jon0	1	1	<1 mm
kar0	1	2	2 mm
kir0	1.5	1	
lek0	1	1.5	
lov0	1	1.5	
mar6	1	1.5	
nor0	1	1.5	
onsa	1	—	Vertical not measured
osk0	1	1	<1 mm
ost0	1.5	1	~<1 mm
	close to 1		
ove0	1.5	3	3 mm !
	excluding 1993: 1		
ske0	3	1	3 mm!
	excluding 2003: 1		
spt0	1	1	<1 mm
sun0	2	1	2 mm
	Excluding 1993: 1		
sve0	1.5	1.5	
ume0	2	4	4 mm !!
		1.5 after 1996	
van0	1	2	2
vil0	1	1	< 1 mm
vis0	3	2	3 mm !
		1 after 1995	

^a Within a square with side length 1, 1.5 or 2 mm.

^b Difference between maximum and minimum value (peak-to-peak).

The plots from ume0 are confusing. First, the horizontal scatter is large (2 mm). It may be noted that the horizontal scatter decrease to slightly more than 1 mm if the measurement in 1995 is excluded. However, we have not found indications of a gross error in the observations that may cause an error at the 1 mm level. In addition, the scatter plot gives equally support for excluding the 1999 measurement. Second, the vertical plot suggests that the pillar has been rising by almost 4 mm since 1993! No reasonable explanation for such an extension of the pillar has been found. If we exclude the first observation 1993, based on the assumption on a gross error in the observations, or some divergent behaviour shortly after its establishment, the remaining measurements fall within slightly more than 1.5 mm.

For vis0 we have a vertical scatter of 2 mm, but if the first measurement in 1993 is excluded, the remaining measurements fall

within 1 mm. The large horizontal motions (3 mm) are interesting. We can not safely explain these displacements. However, we note that this site is located on the island of Gotland where the bedrock consists of limestone (compared to the bedrock of granite or gneiss at other SWEPOS sites). The author has however not sufficient knowledge in geology (or other relevant sciences) to judge to what extent this may contribute to the explanation of the observed displacements.

Based on the results presented in this report, and on the discussion above, it must be concluded that at least some stations in the SWEPOS network may have motions at the level of some few millimetres (2-4 mm). It can also be noted that 2/3 of the sites show maximum scatter of observed monument instability within 1.5 mm (peak-to-peak).

While considering future continuation of the pillar measurements, the disadvantage of the currently used method must be taken into account. The procedure involves removal of the GNSS antenna, placing a total station in the tribrach in order to perform the measurements, and finally replace the antenna. Firstly, this imply interruption in the service from the station, which will cause the network RTK service to be unusable in an area of maybe 100x100 km for some hours. Secondly, the antenna remove-replace may cause shifts in the GPS position time series due to changes in the electromagnetic environment around the antenna (Granström 2006, Johansson et al. 2002, Scherneck et al 2002). Such shifts increase the uncertainty in derived station velocities considerably (e.g. Williams 2003).

The conclusion is that it is recommended to continue the pillar measurement in order to monitor the monument stability. However, it is advised not to continue using the current method but introduce and possibly develop a method that does not include removal of the GNSS antenna. Such a method is used in the GPS network in Finland, FinnRef. See Koivula (2006) for details.

From the pillar measurements performed in 2003, it was noted that some markers in the local networks can no longer be used. Some markers have been destroyed during re-buildings at the station or have been damaged from other causes. Observations to some markers did also show large residuals in the adjustments of the observations. In total 13 out of the 21 sites show damaged markers, large measurement residuals to individual markers, or makes it possible to use a maximum of 4 markers in the local networks. Further investigations of the local networks at these sites (has0, jon0, kar0, lov0, mar6, nor0, onsa, osk0, ost0, ske0, spt0, van0, and vis0) should therefore be considered in order to renovate or otherwise improve the network. Preferably there should be at least 5 available

and well-known markers, forming a good geometry, in order to facilitate safe determination of the pillar reference position also in the future.

5 Acknowledgements

Those who established the local geodetic networks and performed the pillar measurements and computations, as well as those who have contributed with earlier compilations of the pillar measurements, are greatly acknowledged for their efforts.

A number of figures in this report have been created using the Generic Mapping Tool (Wessel and Smith, 1998).

6 References

- Björk K (2000) Formel- och tabellsamling för Teknologi och Konstruktion M. Ågrens Tryckeri AB, Örnsköldsvik.
- Granström C. (2006) Site-Dependent Effects in High-Accuracy Applications of GNSS. Licentiate thesis, Technical report no 13L, Department of Radio and Space Science, Chalmers University of Technology, Sweden.
- Hedling G, and Jonsson B (1993) PREF – a test of a Swedish network of reference stations for positioning. ISSN 0280-5731 LMV-rapport 1993:7.
- Jivall L, Lidberg M (2000): SWEREF 99 –an Updated EUREF Realisation for Sweden. In Torres J A, Hornik H (Eds): Report on the Symposium of the IAG Subcommission for Europe (EUREF) held in Tromsø, 22-24 June 2000. EUREF Publication No 9, 167-175.
- Jivall L (2001) SWEREF 99 – New ETRS 89 Coordinates in Sweden. Lantmäteriet, ISSN 0280-5731 LMV-rapport 2001:6.
http://www.lantmateriet.se/templates/LMV_Page.aspx?id=2688 . Sited Sept. 2007.
- Johansson J M, Davis J L, Scherneck H-G, Milne G A, Vermeer M, Mitrovica J X, Bennett R A, Jonsson B, Elgered G, Elósegui P, Koivula H, Poutanen M, Rönnäng B O, Shapiro I I (2002). Continous GPS measurements of postglacial adjustment in Fennoscandia 1. Geodetic result. J. Geophys. Res., 107(B8), 2157, doi:10.1029/2001 JB000400
- Jonsson B, Hedling G, Jämtnäs L, Wiklund P (2006) SWEPOS Positioning Services – Status Applications and Experiences. Proceedings of the FIG XXIII Congress, 8-13 October 2006, Munich, Germany.
<http://www.fig.net/pub/fig2006/techprog.htm> . Sited July 2007.
- Koivula H, (2006) Implementation and Prospects for Use of a High precision Geodetic GPS Monitoring Network (Finnref)

Covering Finland. Licentiate Thesis, Helsinki University of Technology, Department of Surveying, Espoo.

Nordling C, Österman J (2004) Physics Handbook for Science and Engineering, Seventh edition. Studentlitteratur AB, Sweden. ISBN 9789144044538.

Scherneck H-G, Johansson J M, Elgered G, Davis J L, Jonsson B, Hedling G, Koivula H, Ollikainen M, Poutanen M, Vermeer M, Mitrovica J X, Milne G A (2002) BIFROST: Observing the Three-Dimensional Deformation of Fennoscandia. In Ice Sheets, Sea Level and the Dynamic Earth; Geodynamic series 29; American Geophysical Union.

Wessel P and Smith W H F (1998) New, improved version of Generic Mapping Tools released. EOS Trans. Amer. Geophys. U., vol. 76 (33) pp. 579.

Williams S D P (2003) Offsets in Global Positioning System time series, J. Geophys. Res. 108(B6), 2310, doi:10.1029/2002JB002156.

A. Pillar displacement due to thermal bending

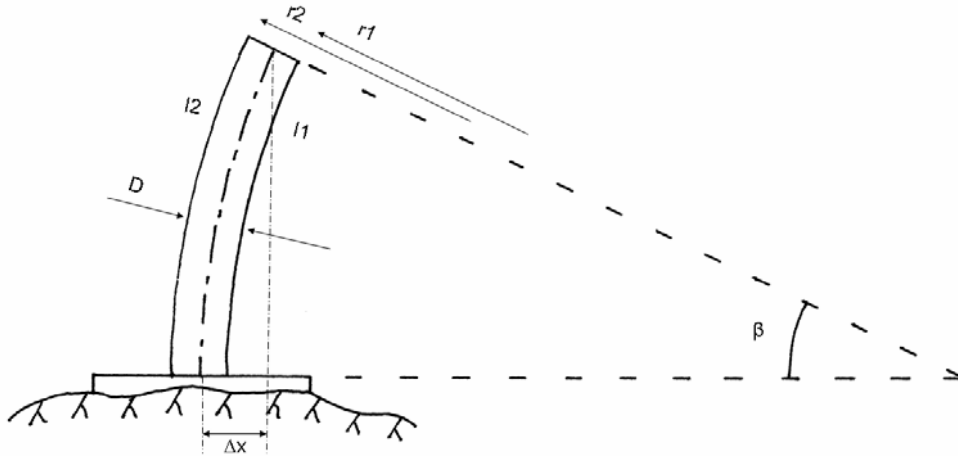


Figure A1. A concrete pillar without insulation exposed to un-even heating (e.g. from sunshine) and thus subject to thermal bending.

Consider an un-insulated concrete pillar exposed to heating from sunshine, which makes one side of the pillar warm and the other side cold. Assume this cause a linear horizontal thermal gradient from right to left in the pillar, where the right side is cool and the left side is warm. Thus the warm side has expanded compared to the cool side. Following the thermal expansion equation, the left side is therefore

$$\Delta l = l \cdot \alpha \cdot \Delta t \quad (\text{A.1})$$

taller compared to the right side. This height difference cause bending of the pillar, and tilting of the pillar top.

It is reasonable to consider the bent pillar to follow the shape of a circle. Figure 1 shows the bent pillar as a segment of a circle with central angle β . The radius and height of the right (inner) and left (outer) side of the pillar are denoted r_1 , l_1 and r_2 , l_2 respectively, and the diameter of the pillar is denoted D . The relation between l , r , and β is given in (A.2 and A3):

Appendix A

$$l_1 = r_1 \cdot \beta \quad (\text{A.2})$$

$$l_2 = r_2 \cdot \beta \quad (\text{A.3})$$

but

$$r_2 = r_1 + D \quad (\text{A.4})$$

and

$$l_2 = l_1 + \Delta l \quad (\text{A.5})$$

(A.4) and (A.5) into (A.3)

$$l_1 + \Delta l = (r_1 + D) \cdot \beta \quad (\text{A.6})$$

(A.6) - (A.2) gives

$$\Delta l = D \cdot \beta \quad (\text{A.7})$$

or

$$\beta = \frac{\Delta l}{D} \quad (\text{A.8})$$

Equation (A.8) can be understood as a tilted pillar top and may be denoted the “pillar top equation” (Figure A2).

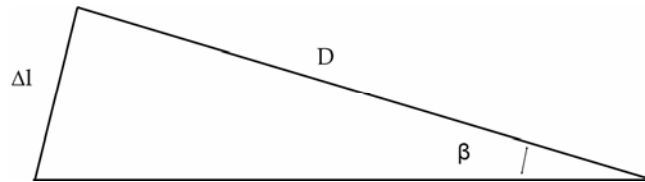


Figure A2. Geometric view of the tilted pillar top.

From (A.2) we get

$$\beta = \frac{l_1}{r_1} \quad (\text{A.9})$$

Into (A.7)

$$\Delta l = D \frac{l_1}{r_1} \quad \Rightarrow \quad r_1 = D \frac{l_1}{\Delta l} \quad (\text{A.10})$$

or

$$r = D \frac{l}{\Delta l} \quad (\text{A.11})$$

which we may call the “radius of curvature equation”.

From Figure A1 we can write the displacement due to bending as:

$$\Delta x = r - r \cdot \cos \beta \quad (\text{A.12})$$

Using $\cos \beta \approx 1 - \frac{\beta^2}{2}$, we can rewrite (A.12) as

$$\Delta x = r(1 - \cos \beta) = r(1 - (1 - \frac{\beta^2}{2})) = r \frac{\beta^2}{2} \quad (\text{A.13})$$

Now use the “pillar top equation” (A.8) and the “radius of curvature equation” (A.11) and input into (A.13)

$$\Delta x = r \frac{\beta^2}{2} = D \frac{l}{\Delta l} \cdot \frac{1}{2} \cdot \left(\frac{\Delta l}{D} \right)^2 = \frac{l}{2} \cdot \frac{\Delta l}{D} \quad (\text{A.14})$$

And substitute using the thermal expansion equation (A.1)

$$\Delta x = \frac{l}{2} \cdot \frac{\Delta l}{D} = \frac{l^2}{2} \cdot \frac{\alpha}{D} \cdot \Delta t \quad (\text{A.15})$$

We may call this equation the “bending displacement equation”.

The pillar top displacement, Δx , is thus proportional to the temperature difference, Δt , between the heated and cooled sides of the pillar, inversely proportional to the diameter, D , of the pillar, and proportional to the square of the height of the pillar.

B. Leica TDA5005 – GDM 440 instrument height difference

04-03-12. Mätning av ΔIH Leica - GDM 440
TDA5005

Leica

VV	Skal-avläsning
100	85,395 cm
300	85,405 cm
300	85,405 cm
100	85,395 cm
	<u>85,400 cm</u>

GDM

VV	Skal-avläsning
100	87,640
300	87,580
100	87,645
300	87,580
	<u>87,611 cm</u>

GDM är $87,611 - 85,400 = 22,11$ mm
högre än Leica

VSB.

Figure B1. Notes from measurements of the difference in instrument height between the Geodimeter 440 and the Leica TDA5005 total stations.

C. T2 - GDM440 instrument heights

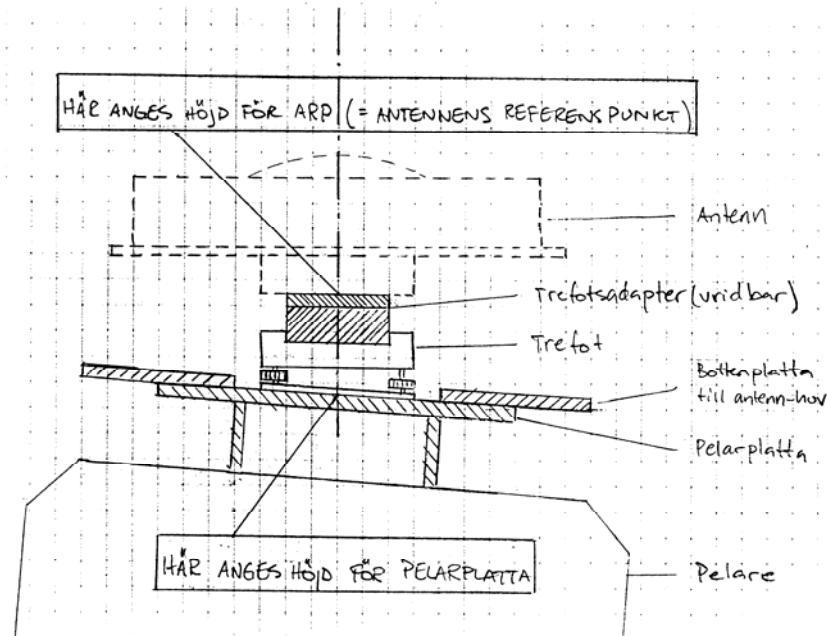
LANTMÄTERIVERKET

Bilaga 2

KG

1993-10-05

Höjdangivelser för SWEPOS-pelare



Höjderna bestäms genom trigonometrisk höjdmätning från pelaren mot avvägda dubbar. Instrumenthöjder är:

	Geodimeter 400	Wild T2	Anm.
Ih över ARP	184.2 mm	162.0 mm	1)
Ih över pelarplatta	255.5 mm	233.3 mm	2) 3)

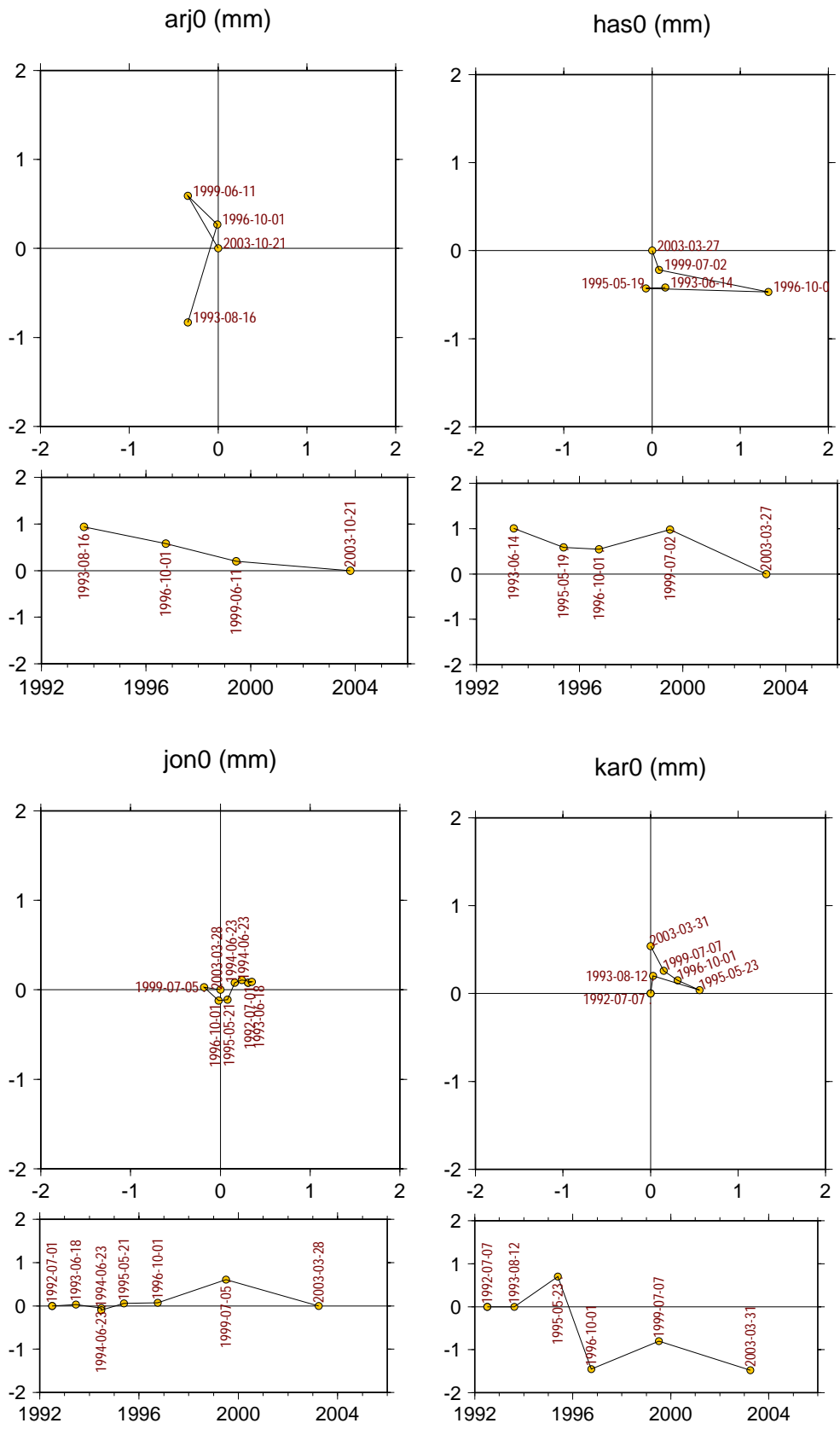
Anm: 1) Avser vridbar adapter.

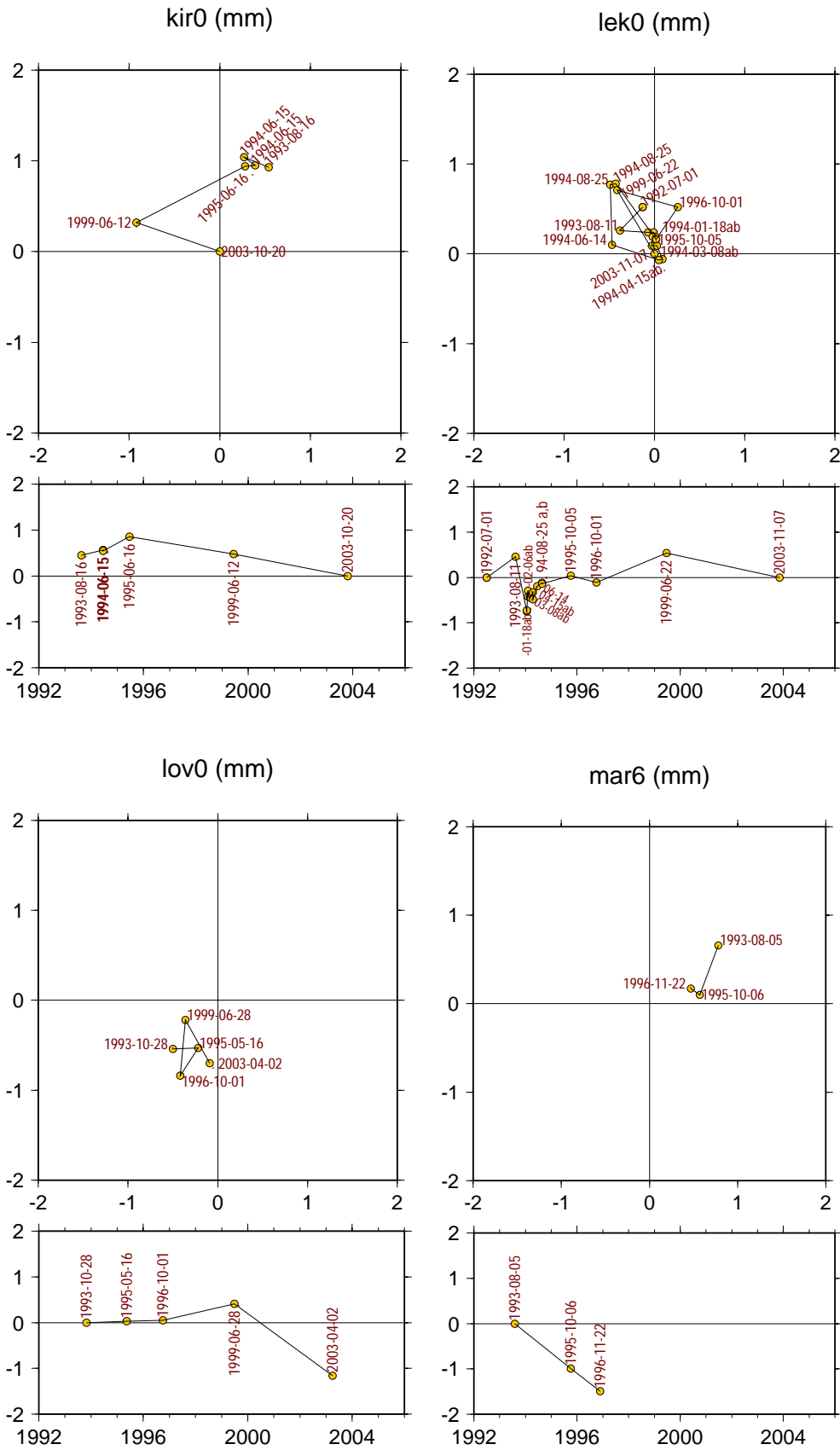
2) Avser horisonterad trefot Wild GDF21/GDF22 i lägsta möjliga läge.

3) En osäkerhet på ± 1 mm finns, p.g.a. att pelarplattornas horisontering varierar.

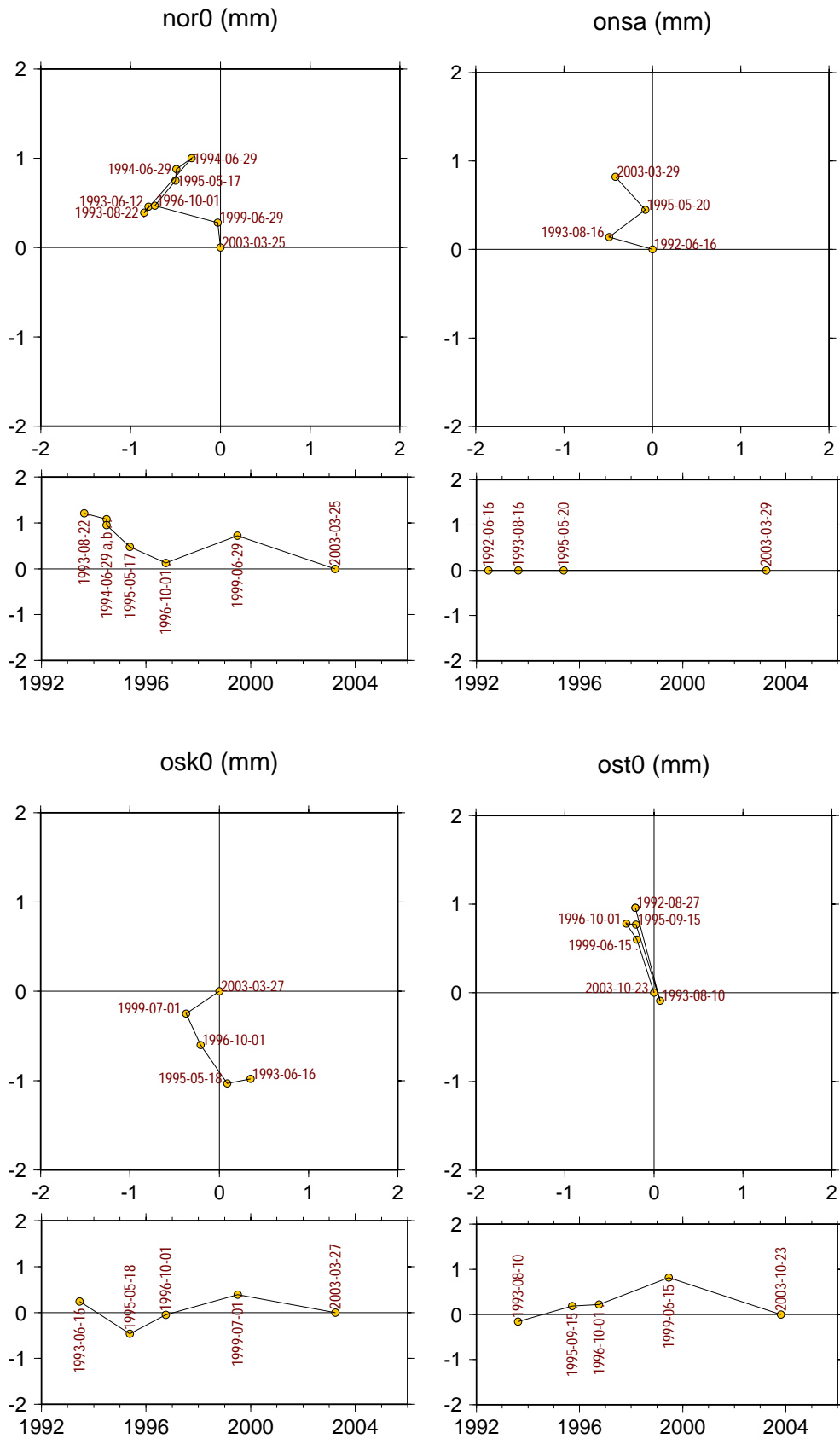
KG>BA>REFSTN>DOK>hojdang.wm

D. Plots of measured displacements of the pillar reference point

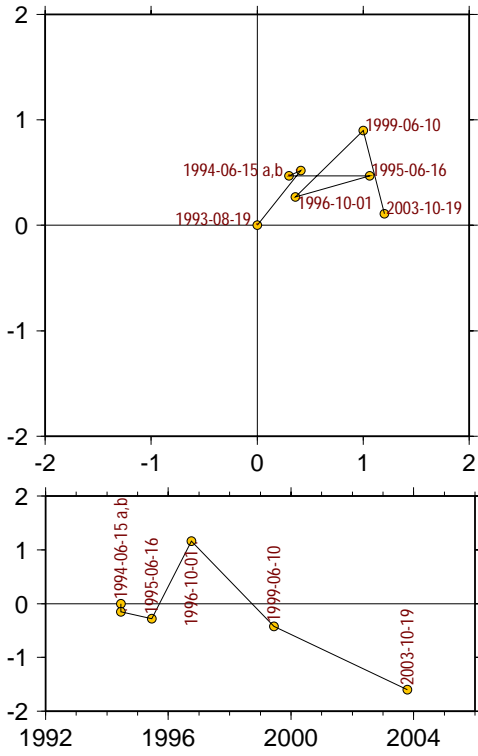




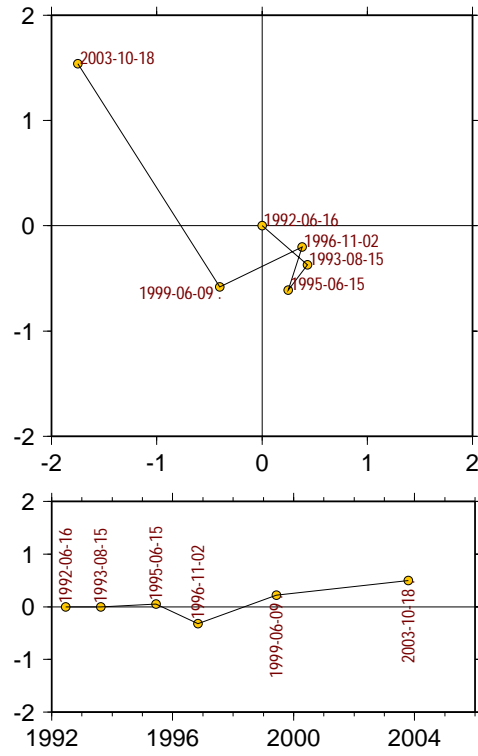
Appendix D



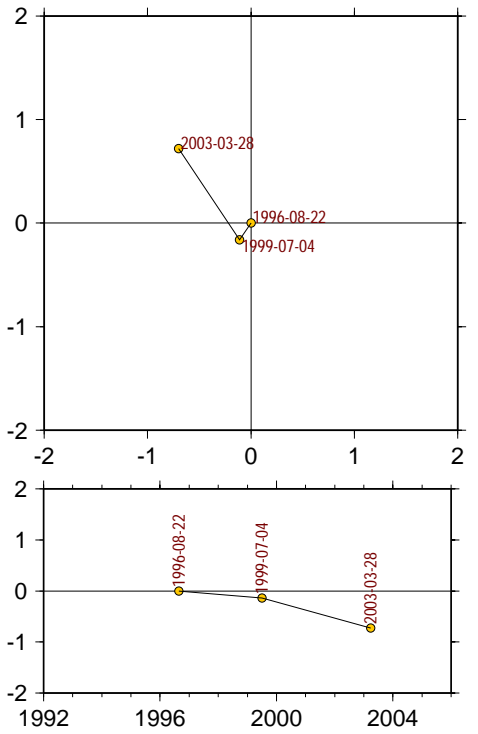
ove0 (mm)



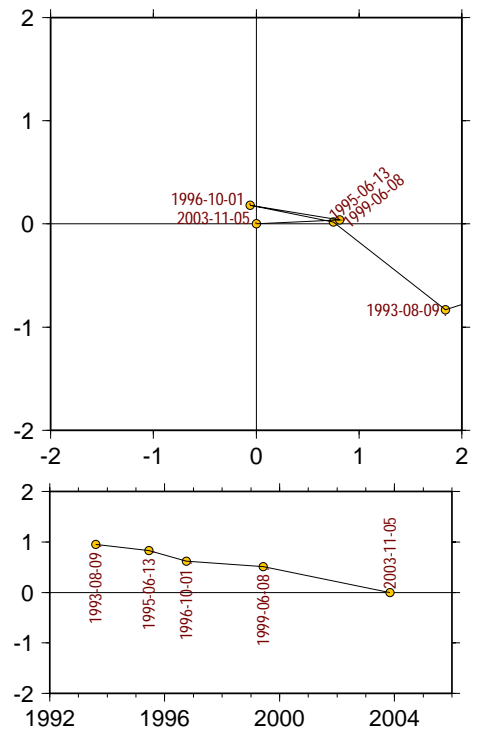
ske0 (mm)



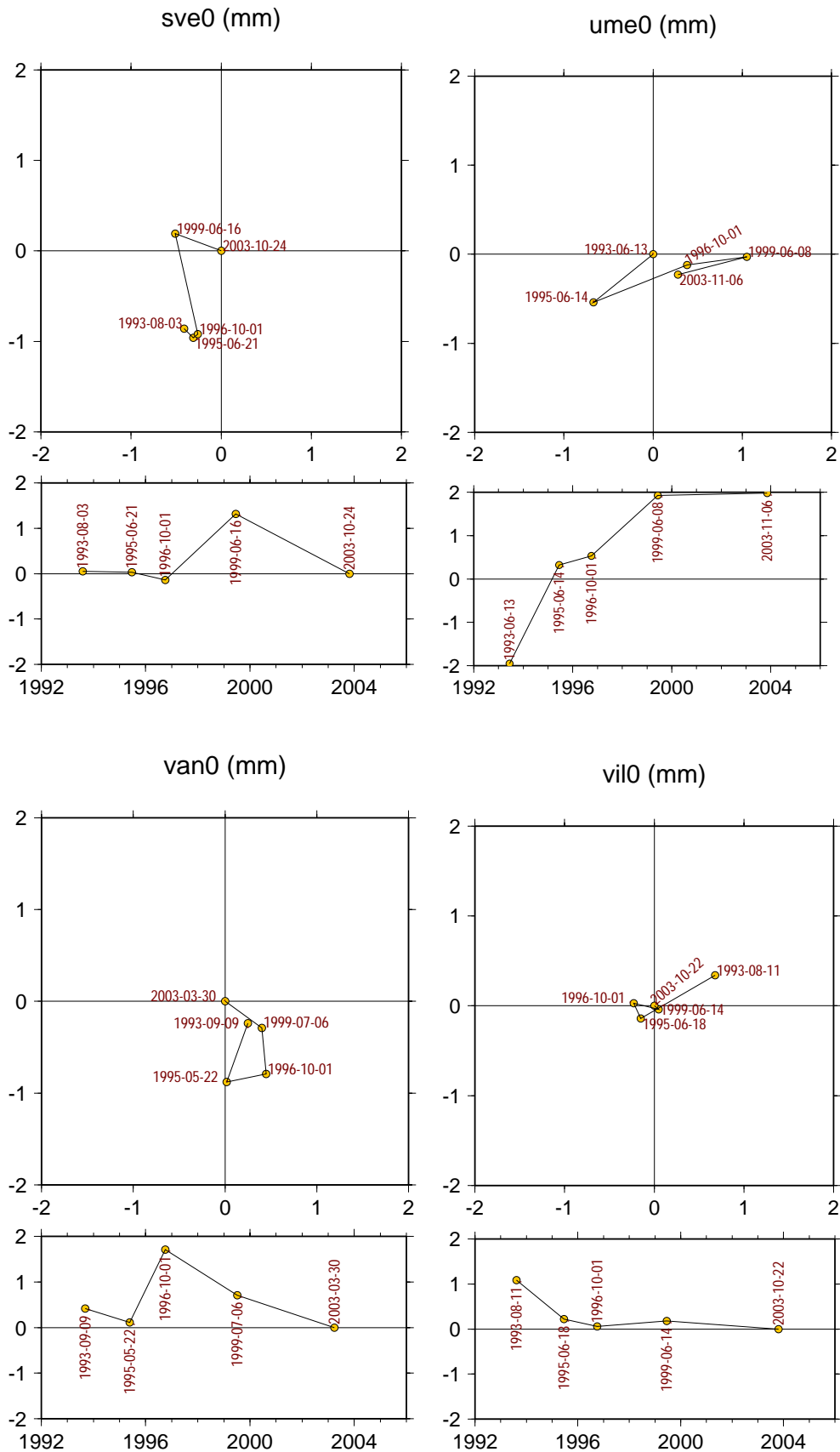
spt0 (mm)



sun0 (mm)



Appendix D



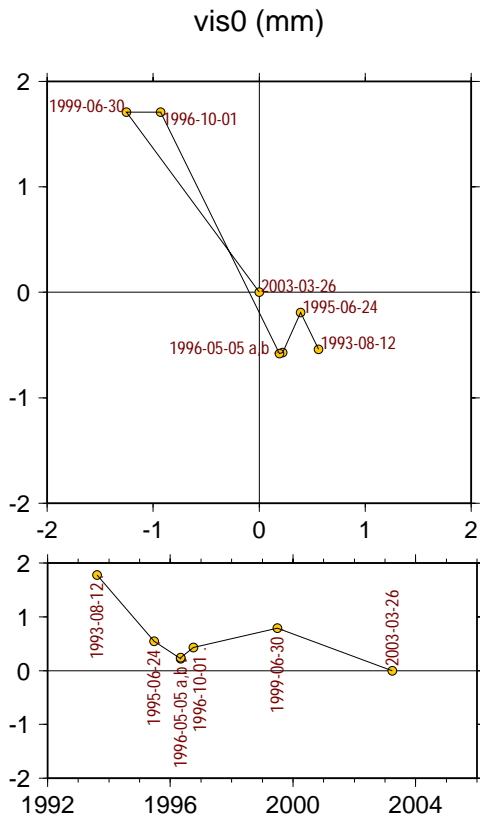


Figure D1. Plots of measured horizontal and vertical displacements of pillar reference points at sites in the SWEPOS network. Unit: mm.

Reports in Geodesy and Geographical Information Systems from Lantmäteriet (the National Land Survey of Sweden)

- 2004:12 Johansson Daniel: SKAN-RTK – 2 – nätverks-RTK i produktionstest i södra Sverige.
- 2004:13 Wiklund Peter: "Position Stockholm-Mälaren – 2" – nätverks-RTK i produktionstest.
- 2004:16 Andersson Therese & Torngren Julia: Traditionell RTK och nätverks-RTK – en jämförelsestudie.
- 2005:3 Ahrenberg Magnus & Olofsson Andreas: En noggrannhetsjämförelse mellan nätverks-RTK och nätverks-DGPS.
- 2005:4 Jämtnäs Lars & Ahlm Linda: Fältstudie av Internet-distribuerad nätverks-RTK.
- 2005:5 Engfeldt Andreas (ed.): Network RTK in northern and central Europe.
- 2005:7 Jivall Lotti, Lidberg Martin, Nørbech Torbjørn, Weber Mette: Processing of the NKG 2003 GPS campaign.
- 2005:8 Eriksson Merja & Hedlund Gunilla: Satellitpositionering med GPS och GPS/GLONASS.
- 2006:2 Norin Dan, Engfeldt Andreas, Johansson Daniel, Lilje Christina: Kortmanual för mätning med SWEPOS Nätverks-RTK-tjänst.
- 2006:3 Klang Dan & Burman Helén: En ny svensk höjdmodell laserskanning, Testprojekt Falun.
- 2006:4 Klang Dan: KRIS-GIS® projekt i Eskilstuna. Kvalitet i höjdmodeller.
- 2006:5 von Malmberg Helena: Jämförelse av Epos och nätverks-DGPS.
- 2006:9 Shah Assad: Systematiska effekter inom den tredje riksavvägningen.
- 2007:1 Johnsson Fredrik & Wallerström Mattias: En nätverks-RTK-jämförelse mellan GPS och GPS/GLONASS.
- 2007:4 Ågren Jonas & Svensson Runar: Postglacial land uplift model and system definition for the new Swedish height system RH 2000.
- 2007:8 Halvardsson Daniel & Johansson Joakim: Jämförelse av distributionskanaler för projektanpassad nätverks-RTK.

L A N T M Ä T E R I E T



Vaktmästeriet 801 82 GÄVLE Tfn 026 - 65 29 15 Fax 026 - 68 75 94
Internet: www.lantmateriet.se